

Influence of the crystal field on the Raman intensity of C₆₀ fullerenes

V. G. Hadjiev* and P. M. Rafailov

Department of Physics, University of Sofia, 1126 Sofia, Bulgaria

H. Jantoljak and C. Thomsen

Institut für Festkörperphysik, Technische Universität Berlin, D-10623 Berlin, Federal Republic of Germany

M. K. Kelly

Walter Schottky Institut, Technische Universität München, D-85748 Garching, Federal Republic of Germany

(Received 2 January 1997)

The Raman-scattering intensity of C₆₀ intramolecular modes in fullerite, excited at 2.41 eV, strongly increases (up to one order of magnitude) upon cooling below room temperature. The effect has different strength for the A_g and H_g modes as well as for predominantly radial (low-frequency) and tangential (high-frequency) modes. The temperature dependence of the Raman intensity suggests that the effect is connected with the orientational ordering of C₆₀ in solids. At low temperature, in the sc phase, the orientational ordering and relatively low site symmetry (S₆) of C₆₀ split the highly degenerate electronic bands. The Raman intensity of the asymmetric H_g modes at resonance turns out to be very sensitive to the band-structure changes due to the vibrational mixing of the electronic bands. We attribute the relatively strong increase of Raman intensity of the radial modes in the sc phase to their more effective modulation of the Coulomb interaction between oriented neighboring C₆₀ molecules. [S0163-1829(97)06729-5]

I. INTRODUCTION

The discovery of superconductivity in alkali-doped C₆₀ fullerenes¹ has drawn additional attention to this remarkable material. Recent theories of phonon-mediated superconductivity in A_xC₆₀ have suggested that Raman-active intramolecular C₆₀ modes might be responsible for the pairing mechanism,^{2,3} which further increases the interest in Raman work on fullerenes and fullerides. Upon cooling pristine C₆₀ solids undergo a first-order transition from a face centered (fcc—space group $Fm\bar{3}m$) to a simple cubic (sc—space group $Pa\bar{3}$) lattice at a temperature near 256 K.⁴ The high-temperature fcc phase is characterized by a rapid free rotation of C₆₀ molecules⁴ which is hindered below 256 K to a ‘‘ratchetlike’’ orientational hopping about [111] directions,^{4,5} and a merohedrally disordered phase is established below 90 K.⁵ Raman-scattering studies from C₆₀ fullerenes initially gave conflicting results^{6–8} that were then found to be due to phototransformation processes that caused creation of dimers or oligomers via a 2+2 cycloaddition in the fcc phase.⁹ These processes can be suppressed when low laser irradiation is used⁶ and dioxygen is present in the lattice.⁹

Modifications of C₆₀ Raman spectra are expected across the phase transition, in particular those connected with changes of the crystal-field symmetry in fullerite. A great deal of Raman work was done on changes that occur in low-temperature Raman spectra, including line splittings and frequency shifts of intramolecular vibrations. These features have been assigned to ¹³C isotope effects,^{10–12} sample disorder¹¹ and to crystal-field effects.^{5,12} With a few exceptions,^{13–15} little attention has been paid so far to C₆₀ Raman intensity changes with temperature, although they are obvious in many of the reported experimental spectra. The

Raman intensity of the C₆₀ modes for *nonresonant* scattering has been calculated within the framework of a bond polarizability¹⁶ and a bond charge¹⁷ model. However, resonant effects are significant when visible laser excitation is used,¹⁸ which invokes their more detailed study.

In this paper we present results regarding the increase in scattering intensity with decreasing temperature of the C₆₀ Raman-active intramolecular phonons in a pure C₆₀ film. In our experiments we used an oxygen-exposed sample to avoid the phototransformation process.^{6,9} We made this compromise because the Raman signal from most of the C₆₀ vibrations was very weak and one needed to use relatively high laser irradiation at conditions that safely prevent the photopolymerization of C₆₀. In addition, it is known that oxygen in crystalline C₆₀ produces almost no measurable change on Raman spectrum relative to that observed in the oxygen-free solid.^{6,9} Finally, oxygen quenches the long-lived, photoexcited triplet state of C₆₀,¹⁹ which is essential for the Raman-scattering analysis done in the present paper: we consider a singlet initial state in the Raman-scattering process.

II. EXPERIMENT

The pure C₆₀ film of thickness 0.4 μm was prepared through evaporation onto silicon substrate in vacuum. For the Raman experiment, the film was first cooled from room temperature to 3 K and then measured at various temperatures. Raman spectra were recorded with a Dilor multichannel spectrometer with slits set to 4 cm⁻¹ spectral width, which along with an absolute accuracy of 1 cm⁻¹, allowed us to resolve numerous fine structures in the Raman lines. The Ar⁺ line at 5145 Å (2.41 eV) was used as an excitation source. The laser power was kept low enough 600 W/cm² that no downshift of the position of the ‘‘pentagonal-pinch’’

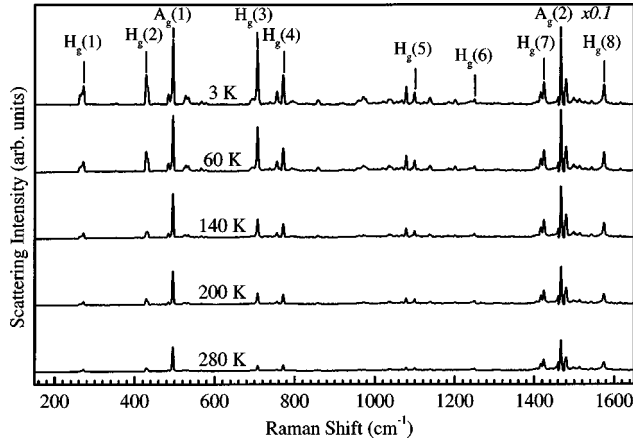


FIG. 1. The Raman spectra of a C_{60} film measured in back-scattering geometry and parallel polarization vectors of scattered and incident light.

A_g mode at 1469 cm^{-1} was observed, a sign that the photopolymerization of the film was avoided.

III. EXPERIMENTAL RESULTS

The group-symmetry analysis for the total vibrational representation of the icosahedral C_{60} structure gives the following direct sum of irreducible representations:¹⁵

$$\Gamma^{\text{vibr}} = 2A_g + 3T_{1g} + 4T_{2g} + 6G_g + 8H_g + A_u + 4T_{1u} + 5T_{2u} + 6G_u + 7H_u. \quad (1)$$

The vector representation Γ^{vect} of the I_h group has T_{1u} symmetry.²⁰ Raman active are phonons with symmetry belonging to $\{\Gamma^{\text{vect}} \otimes \Gamma^{\text{vect}}\} = \{T_{1u} \otimes T_{1u}\} = A_g + H_g$. Therefore the two A_g and the eight H_g modes are Raman allowed by symmetry for the C_{60} molecule. These Raman modes are also expected to be dominant for the van der Waals-bonded molecular C_{60} solids.

In the high-temperature fcc phase (site symmetry T_h), only the Raman-active H_g modes should be split into $E_g + T_g$ modes by the crystal field, because there is only one C_{60} molecule per primitive cell. In the low-temperature sc phase (site symmetry S_6), there are four molecules per primitive cell; A_g and H_g modes should split into $A_g + T_g$ and $A_g + 2E_g + 5T_g$ modes, respectively.²¹ Figure 1 displays Raman spectra of the C_{60} film for five temperatures; the peaks are labeled according to the commonly accepted assignment of Raman-active vibrations of the C_{60} molecule.²²

The most noticeable effect we observed was a large increase in scattering intensity of the C_{60} Raman-active modes with decreasing temperature, especially in the range below the phase transition. In Fig. 2 we plotted the temperature dependence of the quantity

$$I_{\text{rel}}(T) = \frac{I_s(T)}{I_s(300\text{K})} \frac{n_B(300\text{K}) + 1}{n_B(T) + 1}, \quad (2)$$

where $I_s(T)$ is the scattered intensity, determined from the area under the peak, and $n_B + 1$ is the Bose-Einstein factor.

The main experimental observations can be summarized as follows: (i) The Raman intensity of radial type C_{60} vibrations²³ ($100\text{--}800\text{ cm}^{-1}$) increases more strongly with temperature reduction than that of the tangential ones²³ at $1300\text{--}1600\text{ cm}^{-1}$. This comparison only applies to modes with the same symmetry. (ii) The relative intensity increase of the H_g lines is higher than that of the A_g lines. (iii) The intensity of the C_{60} modes changes monotonically with temperature. (iv) The strongest increase of Raman intensity, i.e., the $dI_s(T)/dT$, is not well pronounced around 250 K but instead is shifted to lower temperature. On the other hand, the spectra exhibit qualitatively the same features for all temperatures, except for the appearance of some new lines at low temperature.

We now analyze the reasons for the intensity increase using the complete expression for the Raman signal. The

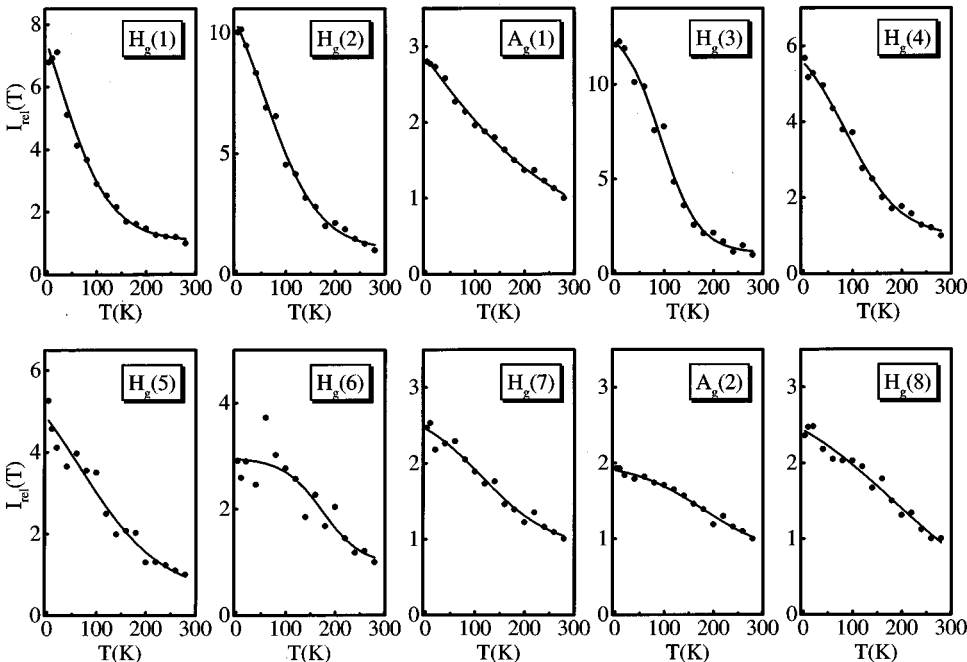


FIG. 2. Temperature dependence of $I_{\text{rel}}(T)$ [see Eq. (2) in the text].

Raman-scattering intensity I_s measured outside the sample and normalized to the incident energy flux is given by

$$I_s = \frac{(1-R)^2}{2\alpha n^2} \frac{\omega_l \omega_s^3}{(4\pi)^2 c^4} |e_l^\rho e_l^\sigma \alpha_{\rho\sigma}(\omega_l - \omega_s, T)|^2 \times \{n_B(\omega_l - \omega_s, T) + 1\}, \quad (3)$$

where R is the reflectivity, α is the absorption coefficient, n is the index of refraction, ω_l and ω_s are the frequencies of incident (laser) and scattered light, e_l^ρ and e_l^σ are the components of their polarization vectors, c is the light velocity, $n_B + 1$ is the Bose-Einstein factor, and $\alpha_{\rho\sigma}$ is the transition susceptibility (Raman tensor). Expression (1) is derived from a more universal representation²⁴ to apply for backscattering geometry and the nontransparency of our C_{60} film to the exciting laser light. We estimated the optical penetration depth δ for the 5145 Å laser line using ellipsometry data available.²⁵ The value of $\delta(5145 \text{ Å}) \approx 0.1 \mu\text{m}$ is smaller than both the film thickness $d \approx 0.4 \mu\text{m}$ and the depth of focus $\delta_f \approx 250 \mu\text{m}$ of our exciting optics, which justifies the use of Eq. (3). The factor $(1-R)^2/2\alpha n^2$ has a relatively weak temperature dependence. We calculated this factor from ellipsometry data and found that it decreases by $\approx 20\%$ from room temperature to 12 K. The absorption coefficient α increases by $\approx 11\%$, but the enhancement of I_s is much stronger in this temperature range, so that the change in α cannot account for the experimental observation.

From Eqs. (2) and (3), neglecting the dependence of $(1-R)^2/2\alpha n^2$ on temperature, it follows that

$$I_{\text{rel}}(T) \approx \frac{|e_s^\rho e_l^\sigma \alpha_{\rho\sigma}|_T^2}{|e_s^\rho e_l^\sigma \alpha_{\rho\sigma}|_{T=300 \text{ K}}^2}. \quad (4)$$

We note here that in our experiment we actually measure the spatially averaged quantity $\langle \alpha_{\rho\rho}^2 \rangle$. For randomly oriented scatterers as microcrystals in our C_{60} film, $\langle \alpha_{\rho\rho}^2 \rangle$ is expressed by the Raman tensor elements after an averaging procedure over all space directions²⁶ as

$$\langle \alpha_{\rho\rho}^2 \rangle = \frac{1}{15} [3(\alpha_{xx}^2 + \alpha_{yy}^2 + \alpha_{zz}^2) + 2(\alpha_{xx}\alpha_{yy} + \alpha_{yy}\alpha_{zz} + \alpha_{zz}\alpha_{xx}) + 4(\alpha_{xy}^2 + \alpha_{yz}^2 + \alpha_{zx}^2)]. \quad (5)$$

Note that in this case all elements of the Raman tensor contribute to the Raman intensity independent of the polarization direction of the incident light. From the above analysis we conclude that the observed temperature behavior of the Raman intensity is mainly governed by a dependence of the Raman tensor components on temperature.

IV. DISCUSSION

Next we discuss the reasons for the change of the polarizability tensor components $\alpha_{\rho\sigma}$ with temperature. A possible mechanism for increasing $\alpha_{\rho\sigma}$ is that the scattering occurs under preresonant or resonant conditions which change with temperature, in particular across a phase transition. Our spectra were excited with the 5145 Å Ar^+ line (2.41 eV), which falls into an absorption region of C_{60} around the first dipole-allowed transition at 2.4–2.7 eV in C_{60} thin films^{25,27}

TABLE I. Symmetry species of the C_{60} intramolecular modes for the isolated molecule (I_h symmetry), the high-temperature fcc lattice and the low temperature phase sc lattice. The indices g and u denote even and odd representations, respectively.

| I_h | fcc phase | sc phase |
|-------------|-----------------------|------------------------------------|
| $A_{g(u)}$ | $A_{g(u)}$ | $A_{g(u)} + T_{g(u)}$ |
| $T_{1g(u)}$ | $T_{g(u)}$ | $A_{g(u)} + E_{g(u)} + 3T_{g(u)}$ |
| $T_{2g(u)}$ | $T_{g(u)}$ | $A_{g(u)} + E_{g(u)} + 3T_{g(u)}$ |
| $G_{g(u)}$ | $A_{g(u)} + T_{g(u)}$ | $2A_{g(u)} + E_{g(u)} + 4T_{g(u)}$ |
| $H_{g(u)}$ | $E_{g(u)} + T_{g(u)}$ | $A_{g(u)} + 2E_{g(u)} + 5T_{g(u)}$ |

and single crystals.²⁸ Resonant excitation profiles have only been studied for the $A_g(2)$ pentagonal-pinch mode at 1468 cm^{-1} by Matus *et al.*²⁹ They determined the Raman resonance for the $A_g(2)$ mode at 2.6 eV. Let us now examine Raman scattering processes in the fcc and sc phases with respect to electronic structure changes at the phase transition.

A. High-temperature C_{60} fcc phase

The ground state of an isolated C_{60} molecule is the totally symmetric spin singlet 1A_g .²⁰ The electron-hole excited $t_{1g}h_u^{-1}$ configuration consists of $t_{1g} \otimes h_u = T_{1u} + T_{2u} + G_u + H_u$ molecular states.²⁰ The dipole operator has T_{1u} symmetry for the I_h structure of the C_{60} molecule, and only transitions to T_{1u} states are dipole allowed from the A_g ground state. The lowest optically allowed transition is at 3.04 eV.³⁰ The calculated energies of some T_{2u}, G_u , and H_u states are between 2 and 3 eV.^{30,31}

In the fcc phase, C_{60} molecules occupy sites of T_h symmetry and the crystal field should split the fivefold highest occupied molecular state, h_u into $e_u + t_u$ states according to Table I (second column). The t_{1g} state and the dipole operator T_{1u} acquire t_g and T_u symmetry, respectively. The molecular states develop into energy bands in solid C_{60} with widths of ≈ 0.5 eV for the fcc phase according to band-structure calculations.^{32,33} The symmetry and degeneracy of the original molecular states are preserved for the Γ point in the Brillouin zone.^{32,33} The degeneracy, however, can be lifted and the symmetry of the wave functions changes at low-symmetry points in the Brillouin zone,^{32,33} and therefore the solid state effect is expected to activate electric-dipole transitions. The possible transitions from the valence band to the t_g band are $t_g e_u^{-1} = t_g \otimes e_u = 2T_u$ and $t_g t_u^{-1} = t_g \otimes t_u = A_u + E_u + 2T_u$. Thus several transitions around the laser excitation including those at the Γ point become dipole-allowed which might contribute to the $A_g(2)$ resonance at 2.6 eV.²⁹ In the fcc phase, however, due to the rapid rotation of C_{60} molecules, the crystal-field effects are smeared out; from NMR experiments³⁴ it follows that the reorientational correlation time is ≈ 9 ps (Ref. 34) at 300 K. We estimated the vibrational lifetime from linewidths and found that it is of the same order. Therefore C_{60} vibrations are localized on individual molecules and the crystal field has a relatively weak effect on them. The rotation of the C_{60} in the fcc phase is also expected to modify and smear out details of the dispersion of the energy bands.³² Recently, Pintschovius *et al.*³⁵ found indications for ordered structures in the high-temperature phase. Interestingly, these structures can hardly

be regarded as a precursor of the 255-K phase transition, because their symmetry differs from that of the low-temperature sc phase. Thus one may conclude that the Raman scattering in the fcc phase is at preresonant conditions for 514 nm excitation, determined by relatively high site symmetry (T_h) of the C_{60} molecules in the lattice and further frustrated by rotational motion.

B. Low-temperature C_{60} sc phase

Below 260 K the C_{60} molecular rotation is hindered. With the establishment of orientational order the number of non-equivalent C_{60} molecules in the unit cell increases to four.⁵ Vibrational and electronic states of C_{60} split according to Table I (third column). Now the valence band, $e_u + t_u$ and the t_g band split into $a_u + 2e_u + 5t_u$ and $a_g + e_g + 3t_g$, respectively. Electronic transitions between these bands lead to the excited states which in terms of an individual C_{60} molecule are given by $(a_g + e_g + 3t_g) \otimes (a_u + 2e_u + 5t_u) = 20A_u + 20E_u + 60T_u$. Note also the increased number of T_u states that can be reached from the valence band to the $a_g + e_g + 3t_g$ band transitions. Orientational hopping of C_{60} in the ‘‘ratchetlike’’ phase below 260 K may smear the crystal-field effects similarly to free rotation in the fcc phase. This may be the reason for shifting the maximum of $dI_s(T)/dT$ to lower temperature than that of the phase transition.

Below we use the Franck-Condon formulation of resonant Raman scattering.^{24,36} Although this is more appropriate for description of Raman scattering of individual molecules, we

assume that it is still valid in the low-temperature phase; the overall character of the vibrational and optical spectra of C_{60} is preserved over the whole range of 300 to 12 K. Raman scattering from the totally symmetric A_g modes is determined mainly by the Franck-Condon (FC) term:^{18,29,36}

$$\alpha_{\rho\sigma}^{\text{FC}} \sim \sum_k \left(\frac{D_{\rho}^o(A_g^o; T_u^e) D_{\sigma}^o(A_g^o; T_u^e) \langle i|k \rangle \langle k|j \rangle}{\omega(T_u^e, k) - \omega(A_g^o, i) - \omega_l + i\gamma} \right), \quad (6)$$

where $D_{\rho}^o(A_g^o; T_u^e) = \langle T_u^e | \wp_{\rho}(T_u) | A_g^o \rangle$ is the electronic transition moment, $\wp_{\rho}(T_u)$ is the ρ th component of the dipole operator, γ is the damping constant for the electronic state e , A_g^o and T_u^e are the electronic wave functions of the ground and excited states, respectively; $\langle i|k \rangle$ and $\langle k|j \rangle$ are the Franck-Condon factors (integrals), with i , j , and k denoting the vibrational wave functions of the ground and resonant states, respectively; $\omega(T_u^e, k)$ and $\omega(A_g^o, i)$ are the frequencies of the resonant and ground vibronic states, respectively.

The Raman intensity of the A_g modes depends on the overlap of the vibrational wave functions of the ground and exciting states and increases when the exciting laser energy ω_l approaches a dipole-allowed transition $[\omega(T_u^e) - \omega(A_g^o)]$. It is noteworthy that in this case Raman intensity does not depend on vibronic mixing of the resonant state e with other states.

The H_g modes are of the Herzberg-Teller type³¹ and their intensity is described by the Herzberg-Teller (HT) term in the total expression for the Raman intensity given in Ref. 27:

$$\alpha_{\rho\sigma}^{\text{HT}} \sim (-1) \sum_{p,k,a} h_{ep}^a \left(\frac{D_{\rho}^o(A_g^o; T_u^p) D_{\sigma}^o(A_g^o; T_u^e) \langle i|k \rangle \langle k|Q_a|j \rangle}{[\omega(T_u^p) - \omega(T_u^e)][\omega(T_u^e, k) - \omega(A_g^o, i) - \omega_l + i\gamma]} + \langle i \leftrightarrow j; \rho \leftrightarrow \sigma \rangle \right), \quad (7)$$

where $h_{ep}^a \sim \langle T_u^p | \partial \hat{H} / \partial Q_a | T_u^e \rangle$ is the perturbation energy per unit displacement of the a th mode that mixes the e and p electronic states, \hat{H} is the electronic Hamiltonian, and Q_a is the displacement operator of the a th mode.

There are several reasons for the stronger increase of the H_g intensity in comparison with that of the A_g modes. First, in contrast to Eq. (6), the factor $[\omega(T_u^p) - \omega(T_u^e)]$ in the denominator in Eq. (7) selects the lowest-lying allowed transitions to state e .³⁶ This may lead to a stronger resonance. In order to illustrate this effect, we focus our attention on the experimentally observed optical transition at 2.35 eV in C_{60} - n -hexane solutions³⁰ which was assigned to the ${}^1A_g \rightarrow {}^1H_u$ transition. As shown above (see Sec. IV A), the ${}^1A_g \rightarrow {}^1H_u$ is one of the possible transitions that leads to the $t_{1g} h_u^{-1}$ configuration. In going from a free C_{60} molecule to the sc phase in solids, H_u states are split and give rise to five T_u states (see Table I). In our experiment we excited Raman spectra with 2.41 eV photon energy which is above the 2.35 eV transition and probably also the transition to the split H_u state. Then according to Eq. (7), the T_u state with the highest energy among the split H_u manifold is in resonance but the remaining four low-lying T_u states will contribute as

well. The FC term given by Eq. (6) which describes the Raman scattering from A_g vibrations selects only one state at resonance.

Second, in the HT term, except for the matrix elements of the allowed optical transitions for which we have $D_{\rho(\sigma)}^o(A_g^o; T_u^e) = \langle T_u^e | \wp_{\rho(\sigma)}(T_u) | A_g^o \rangle \neq 0$ and $h_{ep}^a \neq 0$, optically forbidden Γ^{ht} states coupled to allowed ones via HT active H_g modes can also give a contribution to Raman intensity. For these states one has $\langle \Gamma^{\text{ht}} | \wp_{\rho(\sigma)}(T_u) | A_g^o \rangle = 0$, but $\langle \Gamma^{\text{ht}} | \partial \hat{H} / \partial Q(H_g) | T_u^e \rangle \langle T_u^e | \wp_{\rho(\sigma)}(T_u) | A_g^o \rangle \neq 0$.³⁷ Note that this combination of matrix elements is equivalent to $h_{ep}^a D_{\rho(\sigma)}^o(A_g^o; T_u^e)$ in Eq. (7) and thus contributes to the Raman intensity. For an isolated C_{60} molecule the forbidden states that may couple to the allowed ones are T_{2u}, G_u , and H_u : $T_{2u} \otimes T_{1u} \ni H_g, G_u \otimes T_{1u} \ni H_g$, and $H_u \otimes T_{1u} \ni H_g$. The latter implies that the H_g modes may gain intensity from the HT coupling of forbidden and allowed states. The intensity transfer is maximal when the energy of the coupling mode equals the difference between the forbidden Γ^{ht} and the allowed T_{1u} state.³⁷ In the sc phase, accounting for the splitting of the H_g modes and the H_u and G_u states (see Table I), it follows that the states with A_u and E_u symmetry can

couple to the T_u states via the T_g component of the split H_g modes: $A_u \otimes T_u = T_g$; $E_u \otimes T_u = T_g$. Whenever forbidden states are split in the sc phase and acquire allowed character, the remaining forbidden components still give a contribution to the Raman intensity of the H_g modes. The HT coupling is hardly effective without splitting because the energy interval between neighboring degenerate electronic states is, in principle, bigger than the highest vibrational energy.

Finally, the HT term also includes the perturbation energy per unit displacement h_{ep}^a with $Q_a = Q(H_g)$, where the electronic Hamiltonian \hat{H} is involved. We suggest the following explanation of the experimental observation that the radial mode intensity increases stronger in the sc phase than that of tangential ones. Lu *et al.*³⁸ have proposed a model in which the Coulomb interaction between the neighboring molecules 1 and 2 in fullerite dominates over the thermal energy fluctuations at low temperature and is responsible for the orientational ordering. The Coulomb potential has the form³⁸

$$V_c = \sum_{m,n=1}^{90} \frac{q_m q_n}{|\vec{b}_{1m} - \vec{b}_{2n}|}, \quad (8)$$

where \vec{b}_{1m} and \vec{b}_{2n} are coordinates of bond centers and q_m and q_n are effective bond charges in each of the molecules 1 and 2. This potential should also enter the Hamiltonian \hat{H} . The gradient of V_c is directed along the line connecting the centers of the two molecules, and the distance $|\vec{b}_{1m} - \vec{b}_{2n}|$ is at least 3 Å. Therefore in the low-temperature phase, radial

vibrations modulate \hat{H} more strongly than tangential ones. This gives additional strength *via* h_{ep}^a to the Raman intensity of the radial H_g .

V. CONCLUSIONS

In the present study we demonstrated the complex nature of processes behind the strong increase in Raman intensity of intramolecular modes in C_{60} fullerenes upon lowering temperature. The relatively high site symmetry of C_{60} in the fcc phase, along with rapid free rotation, smear out the crystal-field effects. In the ratchetlike phase below 260 K orientational hopping seems to produce effects similar to that of free rotation. At lower temperature, in the sc phase, the interaction between neighboring C_{60} molecules increases and results in orientational ordering and a lower site symmetry that split highly degenerate electronic states (bands) and vibrations. The Raman intensity of the H_g modes appears to be very sensitive to subtle changes of the band structure because of the specific vibrational mixing of the electronic states (bands).

ACKNOWLEDGMENTS

This work was partially supported by Contracts No. F/312 of the Bulgarian National Science Fund and CIPA-CT93-0032 of the European Community. We thank Björn Pietzak (HMI Berlin) for providing the C_{60} film.

*Present address: Max-Planck-Institut für Festkörperforschung, D-70569 Stuttgart, Germany.

¹A. F. Hebard, M. J. Rosseinsky, R. C. Haddon, D. W. Murphy, S. H. Glarum, T. T. M. Palstra, A. P. Ramirez, and A. R. Kortan, *Nature (London)* **350**, 600 (1991).

²M. Schlüter, M. Lannoo, M. Needles, G. A. Baraff, and D. Tomaneck, *J. Phys. Chem. Solids* **53**, 1473 (1992).

³T. T. M. Palstra and R. C. Haddon, *Solid State Commun.* **92**, 71 (1994).

⁴P. A. Heiney, J. E. Fischer, A. E. McGhie, W. J. Romanow, A. M. Denenstein, J. P. McCauley, Jr., A. B. Smith III, and D. E. Cox, *Phys. Rev. Lett.* **66**, 2911 (1991).

⁵W. I. F. David, R. M. Ibberson, T. J. S. Dennis, J. P. Hare, and K. Prassides, *Europhys. Lett.* **18**, 219 (1992).

⁶P. C. Eklund, P. Zhou, K. Wang, G. Dresselhaus, and M. S. Dresselhaus, *J. Phys. Chem. Solids* **53**, 1391 (1992).

⁷P. H. M. van Loosdrecht, P. J. M. van Bentum, and G. Meijer, *Phys. Rev. Lett.* **69**, 1176 (1992).

⁸V. G. Hadjiev and C. Thomsen, *Phys. Rev. Lett.* **69**, 1146 (1992); P. H. M. van Loosdrecht, P. J. M. van Bentum, and G. Meijer, *ibid.* **69**, 1147 (1992).

⁹P. Zhou, A. M. Rao, K. Wang, J. D. Robertson, C. Eloi, M. S. Meier, S. L. Ren, X. Bi, P. C. Eklund, and M. S. Dresselhaus, *Appl. Phys. Lett.* **60**, 2871 (1992); A. M. Rao, P. Zhou, K.-A. Wang, G. T. Hager, J. M. Holden, Y. Wang, W.-T. Lee, X.-X. Bi, P. C. Eklund, D. S. Cornett, M. A. Duncan, and I. J. Amster, *Science* **259**, 955 (1993).

¹⁰Z.-H. Dong, P. Zhou, J. M. Holden, P. C. Eklund, M. S. Dresselhaus, and G. Dresselhaus, *Phys. Rev. B* **48**, 2862 (1993).

¹¹S. P. Love, D. McBranch, M. Salkolka, N. V. Coppa, J. M. Rob-

inson, B. I. Swanson, and A. R. Bishop, *Chem. Phys. Lett.* **225**, 170 (1994).

¹²L. Akselrod, H. J. Byrne, S. Donovan, and S. Roth, *Chem. Phys.* **192**, 307 (1995).

¹³M. Matus and H. Kuzmany, *Appl. Phys. A* **56**, 241 (1993).

¹⁴V. G. Hadjiev, P. M. Rafailov, C. Thomsen, and M. K. Kelly, in *Physics and Chemistry of Fullerenes and Derivatives*, edited by H. Kuzmany, J. Fink, M. Mehring, and S. Roth (World Scientific, Singapore, 1995), p. 226.

¹⁵H. Kuzmany, M. Matus, B. Burger, and J. Winter, *Adv. Mater.* **6**, 731 (1994).

¹⁶D. W. Snoke and M. Cardona, *Solid State Commun.* **87**, 121 (1993); D. W. Snoke, M. Cardona, S. Sanguinetti, and G. Benedek, *Phys. Rev. B* **53**, 12 641 (1996); S. Guha, J. Menéndez, J. B. Page, and G. B. Adams, *ibid.* **53**, 13 106 (1996).

¹⁷S. Sanguinetti, G. Benedek, M. Righetti, and G. Onida, *Phys. Rev. B* **50**, 6743 (1994).

¹⁸V. N. Denisov, B. N. Marvin, G. Ruani, R. Zamboni, and C. Taliani, *Sov. Phys. JETP* **75**, 158 (1992).

¹⁹J. W. Arbogast, A. P. Darmanyan, C. S. Foote, Y. Rubin, F. N. Diederich, M. M. Alvarez, S. J. Anz, and R. L. Whetten, *J. Phys. Chem.* **95**, 11 (1991).

²⁰R. C. Haddon, L. E. Brus, and K. Raghavachari, *Chem. Phys. Lett.* **125**, 459 (1986).

²¹G. Dresselhaus, M. S. Dresselhaus, and P. C. Eklund, *Phys. Rev. B* **45**, 6923 (1992).

²²D. S. Bethune, G. Meijer, W. C. Tang, H. J. Rosen, W. G. Golden, H. Seki, C. A. Brown, and M. S. de Vries, *Chem. Phys. Lett.* **179**, 181 (1990).

²³D. E. Weeks and W. G. Harter, *J. Chem. Phys.* **90**, 4744 (1989).

- ²⁴M. Cardona, in *Light Scattering in Solids II*, edited by M. Cardona and G. Güntherodt (Springer-Verlag, Berlin, 1982), p. 40.
- ²⁵M. K. Kelly, P. Etchegoin, D. Fuchs, W. Krätschmer, and K. Fostiropoulos, *Phys. Rev. B* **46**, 4963 (1992).
- ²⁶W. Hayes and R. Loudon, *Scattering of Light by Crystals* (Wiley, New York, 1978), p. 113.
- ²⁷S. L. Ren, Y. Wang, A. M. Rao, E. McRae, J. M. Holden, T. Hager, KaiAn Wang, W.-T. Lee, H. F. Ni, J. Selegue, and P. C. Eklund, *Appl. Phys. Lett.* **59**, 2678 (1991).
- ²⁸P. Milani, M. Manfredini, G. Guizzetti, F. Marabelli, and M. Patrini, *Solid State Commun.* **90**, 639 (1994).
- ²⁹M. Matus, H. Kuzmany, and W. Krätschmer, *Solid State Commun.* **80**, 839 (1991).
- ³⁰S. Leach, M. Vervlot, A. Despres, E. Breheret, J. P. Hare, T. J. Dennis, H. W. Kroto, R. Taylor, and D. R. M. Walton, *Chem. Phys.* **160**, 451 (1992).
- ³¹F. Negri, G. Orlandi, and F. Zerbetto, *Chem. Phys. Lett.* **144**, 31 (1992).
- ³²A. Oshiyama, S. Saito, N. Hamada, and Y. Miyamoto, *J. Phys. Chem. Solids* **53**, 1457 (1992).
- ³³N. Laouini, O. K. Andersen, and O. Gunnarsson, *Phys. Rev. B* **51**, 17 446 (1995).
- ³⁴E. D. Johnson, C. S. Yannoni, H. C. Dorn, J. R. Salem, and D. S. Bethune, *Science* **255**, 1235 (1992).
- ³⁵L. Pintschovius, S. L. Charlot, G. Roth, and G. Heger, in *Physics and Chemistry of Fullerenes and Derivatives*, edited by H. Kuzmany, J. Fink, M. Mehring, and S. Roth (World Scientific, Singapore, 1995), p. 39.
- ³⁶A. C. Albrecht, *J. Chem. Phys.* **34**, 1476 (1961).
- ³⁷Y. Yabana and G. F. Bertsch, *Chem. Phys. Lett.* **197**, 32 (1992).
- ³⁸J. P. Lu, X.-P. Li, and R. M. Martin, *Phys. Rev. Lett.* **68**, 1551 (1992).